

# Anaerobic biodegradation of soybean biodiesel and diesel blends under methanogenic conditions



Shuyun Wu<sup>a</sup>, Mohamad H. Yassine<sup>b</sup>, Makram T. Suidan<sup>c,\*</sup>, Albert D. Venosa<sup>d</sup>

<sup>a</sup> Department of Biomedical, Chemical, and Environmental Engineering, University of Cincinnati, Cincinnati, OH 45220, United States

<sup>b</sup> Department of Mathematics and Natural Sciences, College of Arts and Sciences, Gulf University for Science and Technology, Hawally 32093, Kuwait

<sup>c</sup> Faculty of Engineering and Architecture, American University of Beirut, P.O. Box 11-0236, Riad El-Solh, Beirut 1107 2020, Lebanon

<sup>d</sup> U.S. Environmental Protection Agency (retired), National Risk Management Research Laboratory, 26 W. Martin Luther King Drive, Cincinnati, OH 45268, United States

## ARTICLE INFO

### Article history:

Received 10 March 2015

Received in revised form

29 August 2015

Accepted 12 September 2015

Available online 28 September 2015

### Keywords:

Biodiesel

Anaerobic biodegradation kinetics

Petrodiesel

Inhibition

## ABSTRACT

Biotransformation of soybean biodiesel and the inhibitory effect of petrodiesel were studied under methanogenic conditions. Biodiesel removal efficiency of more than 95% was achieved in a chemostat with influent biodiesel concentrations up to 2.45 g/L. The kinetics of anaerobic biodegradation of soybean biodiesel B100 (biodiesel only) with different petrodiesel loads was studied using biomass pre-acclimated to B100 and B80 (80% biodiesel and 20% petrodiesel). The results indicated that the biodiesel fraction of the blend could be effectively biodegraded, whereas petrodiesel was not biodegraded at all under methanogenic conditions. The presence of petrodiesel in blends with biodiesel had a greater inhibitory effect on the rate of biodegradation than the biodegradation efficiency (defined as the efficiency of methane production). Both the biodegradation rate coefficient and the methane production efficiency increased almost linearly with the increasing fraction of biodiesel. With the increasing fraction of petrodiesel, the biodegradation rate and efficiency were correlated with the concentration of soluble FAMES in the water.

© 2015 Elsevier Ltd. All rights reserved.

## 1. Introduction

Biodiesel, a mixture of fatty acid methyl esters (FAMES), with reportedly rapid biodegradation rates, lower acute toxicity (Khan et al., 2007), and a lower carbon dioxide release rate (Hill et al., 2006), is considered a promising alternative to fossil fuels and is gaining widespread acceptance. In the United States, the annual production of biodiesel was 1.28 billion gallons in 2013 and had been increased more than 18-fold since 2005 (Christopher et al., 2014). At present, it is often used in fuel blends with petrodiesel with the volumetric percentage of biodiesel steadily increasing from 7 to 20%. According to the National Diesel Board, the industry has established a goal of using 36 billion gallons biofuel by 2022 (Schnepf and Yacobucci, 2013). The increased demand for biofuel, which involves the processing, transportation, storage, and handling of large quantities of this product, often results in high potential for accidental leaks with a majority of those releases

occurring in subsurface environments having limited dissolved oxygen concentrations. To this end, it is necessary to understand and evaluate the amenability of biodiesel/petrodiesel blends to bioremediation under anaerobic conditions. Aktas et al. (2010) evaluated anaerobic biodegradation of biodiesel in laboratory serum bottles by five anaerobic inocula and found that biodiesel could be easily hydrolyzed and converted to a variety of fatty acid intermediates. They also found that mineralization occurred within one month. To date, most studies on the biodegradation of biodiesel focused on either the anaerobic biodegradation of glycerol as a by-product of the manufacturing of biodiesel or the aerobic biodegradation of biodiesel/petrodiesel blends. Biodegradation of biodiesel and its blends with petrodiesel under anaerobic conditions has rarely been studied.

Little is known about the role of petrodiesel in the biodegradation of biodiesel. In the literature, reports were about how biodiesel blends affect the biodegradation of petrodiesel. Whether the biodiesel would enhance the biodegradation of petrodiesel or not is still being debated and the mechanisms by which it is achieved is inadequately understood. Some studies shown that adding biodiesel could promote and enhance the biodegradation of

\* Corresponding author.

E-mail address: [msuidan@aub.edu.lb](mailto:msuidan@aub.edu.lb) (M.T. Suidan).

petrodiesel. Zhang et al. (1998) and Pasqualino et al. (2006) found that the biodegradability of biodiesel/petrodiesel blends increased with the addition of biodiesel, and they claimed that cometabolism was observed in the biodegradation. Miller and Mudge (1997) observed that in the presence of biodiesel, crude oil exhibited high mobility and a fast rate of microbial degradation, and they suggested that this enhancement was probably achieved through cosolubilization rather than cometabolism. Both DeMello et al. (2007) and Yassine et al. (2013a) have shown that biodegradation of aliphatic hydrocarbons was accelerated in the presence of biodiesel in aqueous system at time scales of days. In addition, studies show the biodegradation rate of the blend increased almost linearly with the increase of biodiesel in the blend, but why the biodegradation rate was correlated to the percentage of biodiesel in the blend was inadequately understood. Some studies have shown that adding biodiesel had no effect or could slow the biodegradation of petrodiesel. Prince et al. (2008) showed that the biodegradation rate of FAMES in petrodiesel/biodiesel blends by unacclimated microorganisms was roughly the same as the biodegradation rate of the n-alkanes. Cyplik et al. (2011) speculated that the bacterial community structure was not affected by the presence of biodiesel because of the structural similarities between fatty acids originating from FAME and oxidized products of alkane biotransformation. Lisiecki et al. (2014) demonstrated that biodiesel does not affect long-term (578 days) biodegradation of aliphatic and aromatic hydrocarbons in saturated sand. Owsianiak et al. (2009) found that for petrodiesel/biodiesel blends of less than 10% biodiesel, the microorganisms preferentially metabolized the FAMES and slowed the assimilation of the n-alkanes. How biodiesel blending would affect the biodegradation of petrodiesel is inadequately understood, and all the studies were conducted only under aerobic conditions. Biodiesel and petrodiesel are both degradable under aerobic conditions. However, petrodiesel alone is resistant to anaerobic biodegradation because it is composed mostly of saturated and aromatic hydrocarbons that exhibit low chemical reactivity. During the past two decades, anaerobic oxidation of petrodiesel constituents has been reported to occur under strict anoxic conditions. A few reports claim observing strict methanogenic biodegradation (Head et al., 2003, Gray et al., 2010). The biodegradation of biodiesel/petrodiesel blends and the effect of petrodiesel on the biotransformation of biodiesel fractions in oil blends under anaerobic conditions have not been investigated up to now.

The objective of this study was to investigate the anaerobic biodegradation of soybean biodiesel blends under methanogenic conditions. Biological methane potential (BMP) tests were conducted in serum bottles to determine the anaerobic biodegradation kinetics of biodiesel in the absence and presence of different concentrations of petrodiesel. The effect of petrodiesel on the biotransformation of biodiesel fractions in biodiesel/petrodiesel blends was determined by partitioning test. Furthermore, the possibility of anaerobic biodegradation of petrodiesel and its inhibition effects on the biodegradation of biodiesel was also investigated.

## 2. Materials and methods

### 2.1. Chemicals

Unblended soybean biodiesel (B100) was purchased from Peter Cramer North America (Cincinnati, OH) with mole fractions of 0.145 palmitic acid methyl ester (C16:0-ME), 0.055 stearic acid methyl ester (C18:0-ME), 0.206 oleic acid methyl ester (C18:1-ME), 0.518 linoleic acid methyl ester (C18:2-ME), and 0.0759 linolenic acid methyl ester (C18:3-ME). Low-sulfur petrodiesel (B0) was

purchased from a local BP petrodiesel station (Cincinnati, OH) with a mole fraction of 0.165 nC10–nC23 n-alkanes, palmitic acid methyl ester (99%), palmitoleic acid methyl ester (99%), stearic acid methyl ester (99%), oleic acid methyl ester (99%), linoleic acid methyl ester (99%), linolenic acid methyl ester (99%), and n-alkanes standard mixture (nC10–nC30), were all purchased from Sigma Aldrich (USA).

### 2.2. Culture acclimation

A 12-L laboratory-scale continuous flow stirred-tank reactor (CSTR) having a 10-L liquid biomass volume and 2-L headspace was inoculated with a bacterial culture, obtained and enriched from an anaerobic digester at a local wastewater treatment plant (Cincinnati Ohio). The bioreactor was operated as a completely mixed system with a solids retention time (SRT) of 40 days. A schematic diagram of the reactor is shown in Fig. 1. A Hamilton syringe pump was used to feed the biodiesel as the sole organic carbon source to the reactor through a buffer solution feed line. The biodiesel concentration in the feed was gradually increased from 0.52 g/L to 2.45 g/L over 15 months. The pH in the chemostat was maintained at  $7.0 \pm 0.20$ . Low pH, nutrient and high pH buffer solutions were provided from separate reservoirs at a total flow rate of 0.25 L/day. The final concentrations of the feed essential nutrients and vitamin minimal medium in the nutrient feed were: 623.25 mg/L  $\text{NH}_4\text{Cl}$ , 196.5 mg/L  $\text{MgCl}_2 \cdot 6\text{H}_2\text{O}$ , 141.662 mg/L  $\text{CaCl}_2 \cdot 2\text{H}_2\text{O}$ , 31.25 mg/L  $\text{FeCl}_2 \cdot 4\text{H}_2\text{O}$ , 416.81 mg/L  $\text{KH}_2\text{PO}_4$ , 9.59 mg/L  $\text{CuSO}_4 \cdot 5\text{H}_2\text{O}$ , 0.32 mg/L  $\text{Na}_2\text{MoO}_4 \cdot 2\text{H}_2\text{O}$ , 13 mg/L  $\text{MnSO}_4 \cdot \text{H}_2\text{O}$ , 10.48 mg/L  $\text{ZnCl}_2$ , 9.16 mg/L  $\text{CoCl}_2 \cdot 6\text{H}_2\text{O}$ , 0.64 mg/L  $\text{B}(\text{OH})_3$ , 9.58 mg/L  $\text{NiCl}_2 \cdot 6\text{H}_2\text{O}$ , 0.24 mg/L 4-aminobenzoic acid (99%), 0.096 mg/L biotin, 0.0048 mg/L cyanocobalamin, 0.096 mg/L folic acid dihydrate (99%), 0.24 mg/L nicotinic acid (98%), 0.24 mg/L pantothenic acid Ca-salt hydrate (98%), 0.48 mg/L pyridoxine hydrochloride (98%), 0.24 mg/L riboflavin (98%), 0.24 mg/L thiamine hydrochloride (99%), 0.24 mg/L thiocetic acid (98%).

### 2.3. Analytical methods

Flow rate of the nutrient and buffer solutions, effluent pH, and total gas production were monitored on a daily basis. The pH was measured using an Orion Model 720 A pH meter (Orion Research, Boston, Massachusetts). COD was measured using Hach Method 8000 on a Hach DR/200 Spectrophotometer (Hach, Loveland, Colorado). Gas composition was analyzed on a weekly basis for  $\text{CH}_4$ ,  $\text{CO}_2$ ,  $\text{O}_2$  and  $\text{N}_2$ . Analysis for gas composition was performed on an

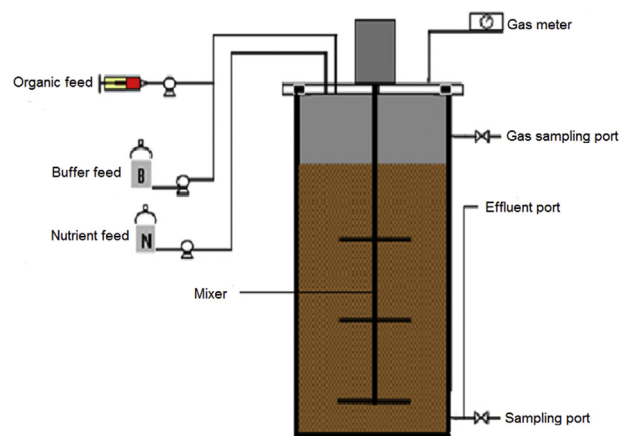


Fig. 1. Schematic of chemostat.

HP5890 Series II Gas Chromatograph (GC) (Hewlett Packard, Wilmington, Delaware) equipped with a thermal conductivity detector (TCD) using an HP 10-ft molecular sieve BX-45/60 mesh HP 6 ft HAYESE PQ 80/100 column (Supelco, Bellefonte, Pennsylvania). VFAs were measured on an Agilent 6890 II GC equipped with a flame ionization detector (FID) using 2 mm i.d. 1.83 m glass column packed with 4% Carbowax on a 80/120 Carbowax B-DA (Supelco, Bellefonte, Pennsylvania). Liquid samples, collected weekly from the sampling port, were filtered through 0.45  $\mu\text{m}$  filters and analyzed for the target compounds, VFAs, and effluent chemical oxygen demand (COD). FAMES and n-alkanes in the effluent were extracted and analyzed on an Agilent 6890 II GC equipped with a HP-INNOWAX capillary column (30 m, 0.25 mm i.d., 0.25  $\mu\text{m}$  film thickness), and an Agilent 5973 Mass Spectrometer Detector (MSD). The flow rate of the carrier gas helium was 1 ml/min, the temperature of inlet and detector interface was set at 320 °C, and the inlet was operated in splitless mode. Oven temperature program was set as follows: hold at 35 °C for 3 min, ramp at 5 °C/min to 250 °C and hold at 250 °C for 5 min.

#### 2.4. BMP tests

The BMP tests followed the procedure outlined by Gupta et al. (1996). Once the chemostat reached steady state, i.e., several consecutive measurements revealed consistently low effluent concentrations of the target compounds and effluent COD, and methane gas production was stable and near expected values, biomass was collected from the reactor and used as a source culture for the BMP test. 60-ml serum bottles were sterilized, surface-deactivated and placed in an anaerobic hood. Inside the hood, each bottle was filled with 20 ml of chemostat effluent (which contained the anaerobic biomass), 20 ml of nutrient and buffer solution and 20 ml  $\text{N}_2$  headspace. 0.3 mg/L Resazurin was used as an indicator of anaerobic conditions. The nutrient solution was purged for about 5 h with nitrogen gas prior to placing it in an anaerobic chamber for 3 days to remove any trace oxygen in the solution. After addition of the various solutions, each serum bottle was capped with Teflon (Supelco) and spiked with 15  $\mu\text{l}$  biodiesel containing different volume petrodiesel loads (0, 0.5, 1, 2.5, 5, 7.5, 15, 30 and 45  $\mu\text{l}$ ). A separate set of bottles was injected with only petrodiesel. Killed control samples were prepared the same way except the effluent was autoclaved at 121 °C for 60 min. In addition to the biotic and abiotic samples, three blank control samples were prepared with only nutrient and effluent solutions with no injection of any biodiesel and petrodiesel. All experiments were done in triplicate and were performed at room temperature 22 °C. A total of 10 biologically active events, three biomass control events (without spiking oil), and three killed control events (abiotic controls) were prepared. Serum bottles were sealed and placed in a tumbler. Sampling was performed at different time intervals, the volume of gas produced was measured, and gas composition of the headspace was analyzed to calculate the volume of methane produced. At the end of the BMP tests, the liquid phase was completely liquid–liquid extracted with dichloromethane. The extracts were filtered through anhydrous sodium sulfate to dewater them and stored at –20 °C until analysis on GC–MS.

#### 2.5. Partitioning experiment

Super-Q water was purged with nitrogen gas for 5 h before being placed into the anaerobic chamber and set there for two days to remove any remaining trace concentrations of dissolved oxygen. Each 160 ml serum bottle was filled with 120 ml Super-Q water and then sealed and spiked with 45  $\mu\text{l}$  biodiesel containing

different petrodiesel fractions (0, 1.5, 3, 7.5, 15, 22.5, 45, 90 and 135  $\mu\text{l}$ ). This represented the same oil/water volume ratio as in the BMP batch test. Serum bottles were then placed in a tumbler. After 24 h mixing, samples were then transferred to 125 ml glass separatory funnels and allowed to settle for 3 h 50 ml of the WAFs were withdrawn from the bottom of the funnels and were completely liquid–liquid extracted with 25 ml dichloromethane (DCM). The extracts were filtered through anhydrous sodium sulfate to dewater them and then concentrated 10-fold in a TurboVap II Evaporation System. Samples were analyzed on the GC–MS.

### 3. Results and discussion

#### 3.1. Chemostat steady-state operation

The startup period for the reactor lasted six months and the organic feed concentration was progressively increased from 0.52 g/L to 1.4 g/L. Once the 1.4 g/L feed concentration was reached, reactor operation was continued until conditions stabilized. The feed was then increased to a higher concentration and again allowed to stabilize. This process was repeated until the final feed concentration of 2.45 g/L was reached. Fig. 2 shows the weekly COD balance for the chemostat after six months of operation with the organic feed ranging from 1.75 g/L to 2.45 g/L. The GC/MS analysis indicated that the extent of FAMES removal at any influent concentration was more than 95%. The influent COD was in the form of soybean biodiesel B100, and the effluent COD was the soluble COD in the effluent, mainly attributable to the biodegradation intermediate, acetic acid. The difference between the influent COD and the effluent COD + methane COD are the fraction of the COD that is utilized for biomass production, volatilized acetic acid and solidified biodiesel. After day 502 of operation, the reactor was fed a blend of biodiesel (80%) and petrodiesel (20%), B80. Effluent chemical analysis revealed that the petrodiesel fraction was not biodegraded and accumulated in the reactor. Methane production decreased to the expected methane production as if biodiesel were the only substrate utilized. The difference between the influent COD and the effluent COD + methane COD was mainly the COD attributable to the undegraded petrodiesel fraction in the blend, the COD that is consumed in biomass production and lost due to volatilized acetic acid and solidified biodiesel.

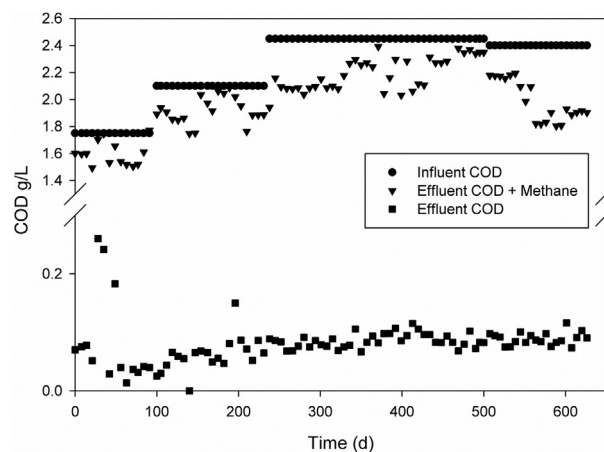


Fig. 2. Weekly COD balance for chemostat.

### 3.2. Biodegradation kinetics

The first biochemical methane potential (BMP) test was performed using 15  $\mu$ l of biodiesel B100 per bottle supplemented with different volumes of petrodiesel. Biomass used for this test was acclimated to soybean biodiesel B100 only. The test was performed to assess the effect of the presence of different volumes of petrodiesel loads on the rate of anaerobic biodegradation of soybean biodiesel. Biodegradation was monitored through methane production, and the cumulative methane production curves obtained for the different petrodiesel treatments are presented in Fig. 3. In all treatments, methane production curves followed a biodegradation profile of a typical apparent biomass exponential growth approaching a plateau level. The achieved cumulative methane production ( $M_t$ ) decreased with increasing petrodiesel fractions. In order to quantify the biodegradation of biodiesel through methane production in the biotic microcosms with different petrodiesel loads, first-order biodegradation rate constants were calculated using Equation (1):

$$M_t = M_u(1 - e^{-kt}) \quad (1)$$

where,

$M_t$  = cumulative methane produced (ml) at time  $t$ ,  
 $M_u$  = ultimate methane production (ml),

$k$  = first order biodegradation rate constant ( $d^{-1}$ ).  
 $T$  = time (d).

The  $k$  and  $M_u$  values were estimated by nonlinear least-squares regression using SigmaPlot 11 (systatsoftware, Inc., CA) by fitting the experimentally determined cumulative methane production data rather well as shown in Figs. 3 and 4, with methane production and first-order rate coefficients listed in Table 1. The first-order rate coefficient was  $0.15 \pm 0.0088/d$  for biodiesel B100 alone. In response to the injection of varying petrodiesel loads, the first-order rate coefficient decreased with the increasing amounts of petrodiesel. The volumes of petrodiesel injected with the 15  $\mu$ l of biodiesel were 0, 0.5, 1, 2.5, 5, 7.5 and 15  $\mu$ l, which resulted in an influent volume fraction of biodiesel of 1, 0.97, 0.94, 0.86, 0.75, 0.67 and 0.50. The first-order biodegradation rate constant increased with the increasing volume fraction of biodiesel. The first-order rate constants for biodiesel biodegradation are plotted in Fig. 5 against the corresponding biodiesel volume fraction. The figure shows a good linear correlation between the first-order biodegradation rate constant and the volume fraction of biodiesel, with the linear relationship having a slope of  $0.11 \pm 0.001$ .

The theoretical methane production of 15  $\mu$ l biodiesel was calculated by measuring the COD of the biodiesel, which is 2.75 g COD/g biodiesel, which corresponds to a methane production of 13.78 ml. The observed methane production in response to the

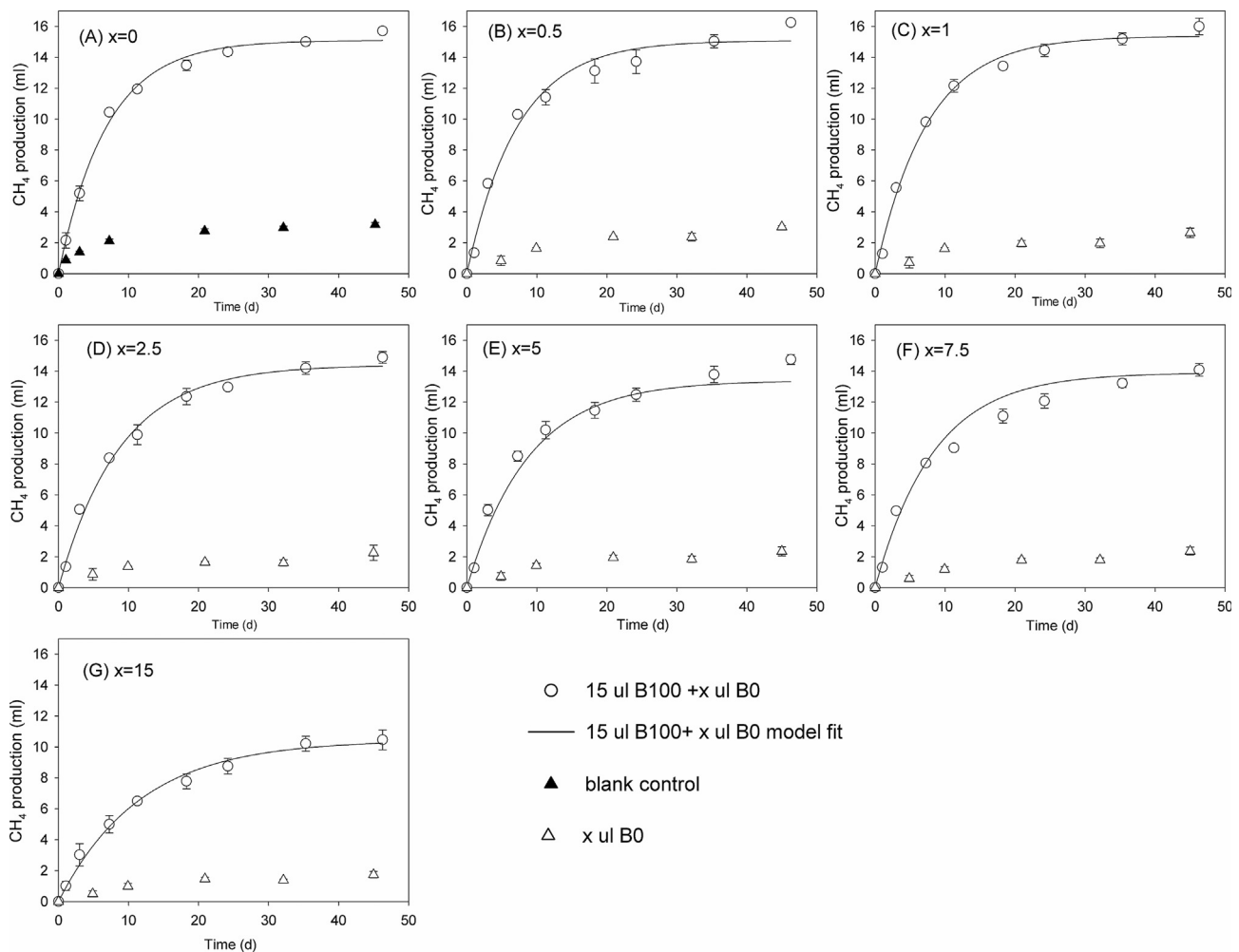
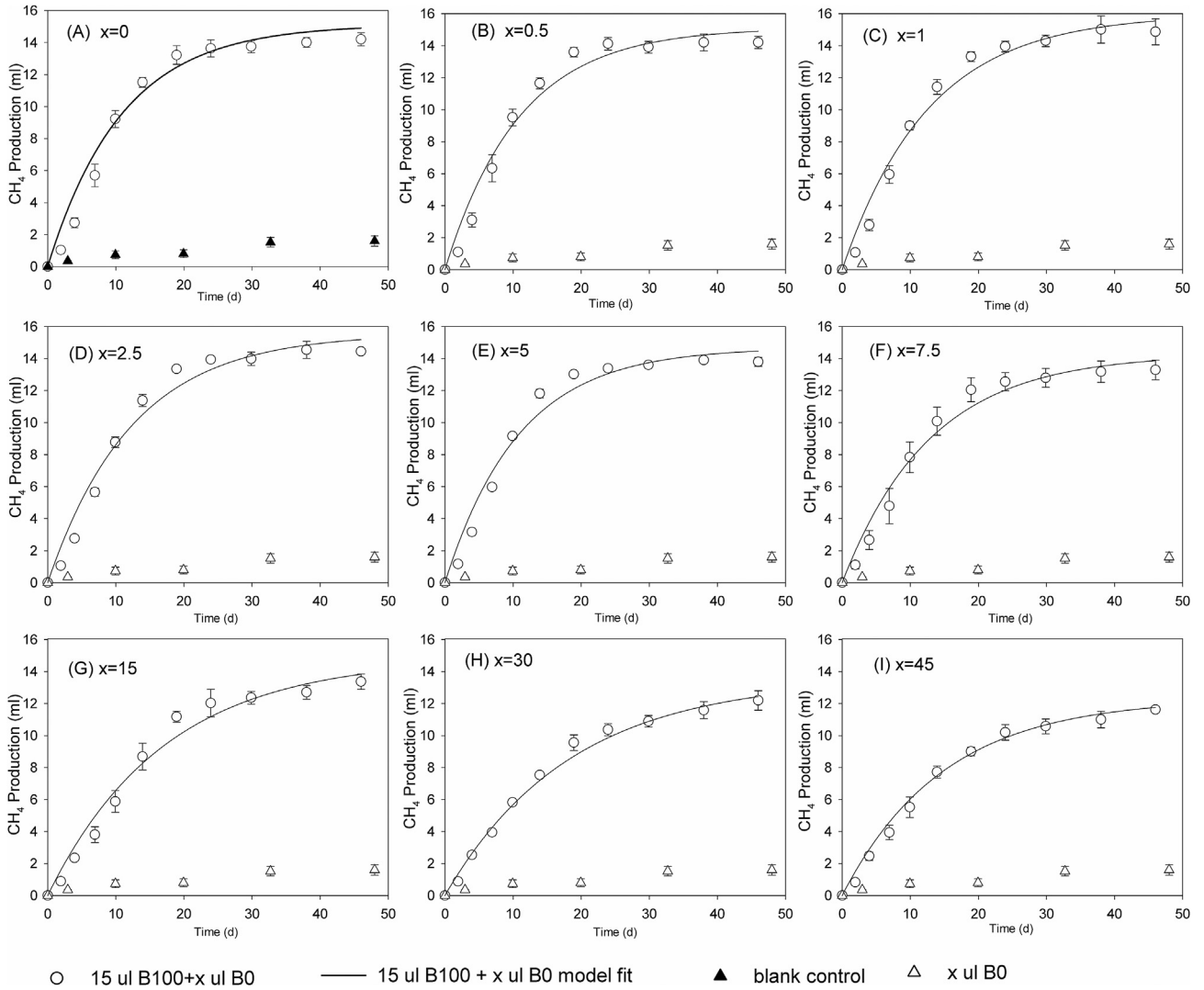


Fig. 3. Cumulative  $CH_4$  production curves for soybean biodegradation with different B0 loads using culture from reactor B100, points are triplicate experimental data while the solid line is model fit equation.



**Fig. 4.** Cumulative CH<sub>4</sub> production curves for soybean biodiesel biodegradation with different B0 loads using culture from reactor B80, points are triplicate experimental data while the solid line is model fit equation.

**Table 1**

Methane production of 15 µl soybean biodiesel with different volume loads of petrodiesel and nonlinear regression parameters for methane production curves using culture from reactor B100 and B80.

Added B0 (µl)	Culture from reactor B100		Culture from reactor B80	
	CH4 exp (ml)	k (d <sup>-1</sup> )	CH4 exp (ml)	k (d <sup>-1</sup> )
0	15.70 ± 0.19	0.15 ± 0.0088	14.20 ± 0.41	0.086 ± 0.012
0.5	16.24 ± 0.14	0.14 ± 0.016	14.20 ± 0.38	0.092 ± 0.012
1	15.06 ± 0.53	0.14 ± 0.010	14.86 ± 0.81	0.079 ± 0.009
2.5	14.89 ± 0.37	0.13 ± 0.009	14.44 ± 0.072	0.081 ± 0.011
5	14.76 ± 0.32	0.12 ± 0.012	13.79 ± 0.28	0.092 ± 0.012
7.5	13.09 ± 0.40	0.11 ± 0.013	13.28 ± 0.62	0.077 ± 0.010
15	10.46 ± 0.68	0.086 ± 0.008	13.36 ± 0.48	0.059 ± 0.009
30	—	—	12.16 ± 0.59	0.060 ± 0.043
45	—	—	11.61 ± 0.18	0.063 ± 0.009

CH<sub>4</sub> exp, experimental methane production ± standard deviation among three replicates; k, first order rate constant ± standard error.

injection of 15 µl biodiesel is that observed from the experiment minus that produced in the biomass controls. The methane produced in response to injection of 15 µl biodiesel is shown in Table 2. With the increase in petrodiesel loads, the methane production decreased possibly due to a decrease in the bioavailability of soluble

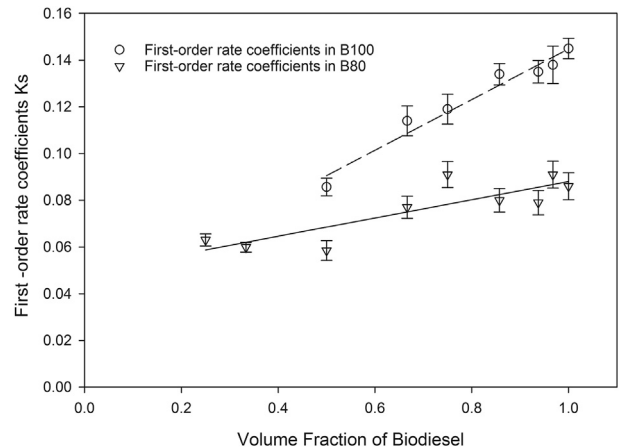


**Fig. 5.** First-order rate coefficients in different volume fraction biodiesel.

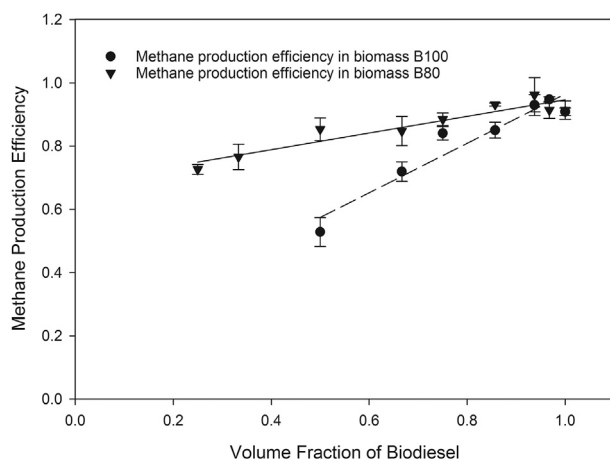
FAMES in the water and the toxicity of the added petrodiesel. Yassine et al. (2012) examined the microtox toxicity of the water accommodated fraction (WAF) of six soybean biodiesel and

**Table 2**15  $\mu\text{l}$  soybean biodiesel B100 methane production efficiency using culture from reactor B100 and B80.

Added B0 ( $\mu\text{l}$ )	CH <sub>4</sub> production in culture B100 (ml)	CH <sub>4</sub> production in culture B80 (ml)
0	12.526	12.599
0.5	13.065	12.602
1	12.818	13.265
2.5	11.719	12.840
5	11.586	12.194
7.5	9.915	11.682
15	7.286	11.761
30	—	10.556
45	—	10.011

petrodiesel blends at different oil loads and observed that EC 50 for B0 was around 11.52 to 20 at different dilutions from 1:1 to 1:1000. Methane production corresponding to injection of only 15  $\mu\text{l}$  pure biodiesel was 91% of the expected value. There was no significant difference ( $p = 0.8$ ) in the ultimate methane produced when lower petrodiesel volume fractions were added, i.e.,  $\leq 1 \mu\text{l}$ . The methane production efficiency was greater than 85% of theoretical for the bottles where the added petrodiesel volumes were between 0 and 5  $\mu\text{l}$ . Over the whole range, the methane production efficiency increased linearly with the fraction of biodiesel as shown in Fig. 6, the linear rate of increase was  $0.78 \pm 0.10$ . The first order rate constant for the biodegradation of biodiesel in the absence of any petrodiesel was  $0.15 \pm 0.0088 \text{ d}^{-1}$ . The first order rate constant decreased to  $0.086 \pm 0.008 \text{ d}^{-1}$  when 15  $\mu\text{l}$  of petrodiesel was added to the mix. Hence, in the presence of 15  $\mu\text{l}$  petrodiesel, the biodiesel first order biodegradation rate constant decreased to 59% of the observed value when no petroleum biodiesel was present. The biodegradation efficiency was decreased by a factor of 58% when compared to the case when no petrodiesel was added. The data are summarized in Table 2 and Figs. 5 and 6.

No methane production was observed in any of the killed control samples. Small amounts of methane were produced in blank biomass control samples (triangle symbols in part A of Figs. 3 and 4). This methane production was likely due to the biodegradation of residual organic matter in the chemostat effluent. Similar behavior was observed in the petrodiesel alone treatments (open triangle symbols in Figs. 3 and 4). However, in all cases, methane production in the petrodiesel only treatments was lower than that in the biomass blank control samples. Consequently, there was no methane production when petrodiesel was present alone, suggesting that petrodiesel was not biodegraded under methanogenic conditions. This supports the results that methane produced in the biodiesel and petrodiesel blends was due only to biodiesel

**Fig. 6.** Methane production efficiency in different volume fraction biodiesel.

biodegradation. The data in Table 2 suggest that the final methane produced when 1  $\mu\text{l}$  of petrodiesel was added to 15  $\mu\text{l}$  of biodiesel was slightly greater than that observed for biodiesel alone. Similar behavior was observed in the second BMP test when 0.5, 1, and 2.5  $\mu\text{l}$  of petrodiesel was added. This might be attributed to stress induced by the presence of petrodiesel that may affect the portion of the substrate transformed to biomass.

To further investigate the effect of petrodiesel on the biodegradation of biodiesel and to assess the possibility of co-metabolism, the feed to the chemostat was modified to a volume fraction of 80% biodiesel and 20% petrodiesel. After two SRT turnovers, stable methane production was reestablished. Effluent from this chemostat was used to conduct a second BMP test with petrodiesel volume added similarly to the first BMP test, except in this case two additional petrodiesel volumes of 30 and 45  $\mu\text{l}$  were tested, corresponding to volume fractions of biodiesel of 0.33 and 0.25, respectively. The biodegradation rate coefficients were calculated by fitting the data to the first-order model Equation (1). The mathematical model fit the experimental data very well as shown in Fig. 4, with final methane production and first-order biodegradation rate coefficients listed in Table 1. The first-order biodegradation rate coefficients were significantly decreased after the biomass was acclimated to B80 when compared to the results obtained from the test using culture from the chemostat operated on a feed of biodiesel alone ( $p = 0.0003$ ). This suggests that the activity of the culture was inhibited by the presence of petrodiesel in the feed. The first-order rate constant was  $0.086 \pm 0.012 \text{ d}^{-1}$  when pure 15  $\mu\text{l}$  biodiesel was added compared to  $0.15 \pm 0.088 \text{ d}^{-1}$  obtained from the BMP test using biomass B100. However, the differences in the value of the first order rate constant for the different petrodiesel added volumes decreased suggesting that the bulk of the inhibitory effect of petrodiesel was absorbed in the biomass that was acclimated to the presence of petrodiesel. The first-order rate constant when 15  $\mu\text{l}$  of petrodiesel added was  $0.059 \pm 0.009 \text{ d}^{-1}$ , which is 68% of the value observed when no petrodiesel was injected, while the biodegradation efficiency was decreased to 85%. When these values are compared to the 59 and 58% obtained from the BMP test using biomass B100, it again supported the conclusion that the presence of petrodiesel in the reactor feed resulted in a culture that was acclimated to the presence of petrodiesel and, therefore, less susceptible to further inhibition. This supports the findings in the first BMP test that the presence of petrodiesel had a greater effect on the rate rather than extent of biodegradation. Observed differences were lower in biodegradation efficiency when the petrodiesel load varied from 0  $\mu\text{l}$  to 2.5  $\mu\text{l}$ , and the ultimate methane production efficiency was greater than 85% for petrodiesel loads up to 15  $\mu\text{l}$ . Similar to the results observed in the first BMP test, both the first-order biodegradation rate constant and the methane production efficiency increased linearly with the increasing volume fraction of biodiesel as shown in Figs. 5 and 6, the linear rates of increase were  $0.78 \pm 0.10$  and  $0.22 \pm 0.035$ , compared to the linear rate  $0.11 \pm 0.001$  and  $0.0039 \pm 0.009$  in the first BMP test.

### 3.3. Biodiesel bioavailability

In the presence of biodiesel, we expected the readily biodegraded constituents of biodiesel to serve as the primary substrate in the anaerobic co-metabolism of petrodiesel constituents, but the results showed that the biodegradation of petrodiesel did not occur under methanogenic conditions. However, the initial rate of transformation of the FAMES appears to be influenced by the amount of petrodiesel in the blends. Both the biodegradation rate

and methane production efficiency increased almost linearly with the increasing fraction of biodiesel. This is consistent with observations made by Zhang et al. (1998) under aerobic conditions. They claimed that biodiesel increased the biodegradability of biodiesel/petrodiesel blends by co-metabolism. However, co-metabolism was confirmed did not occur in this study. Other study when biodiesel was observed enhance the biodegradation of crude oil, they suggested that it was probably achieved through co-solubilization because in the presence of biodiesel, crude oil exhibited high

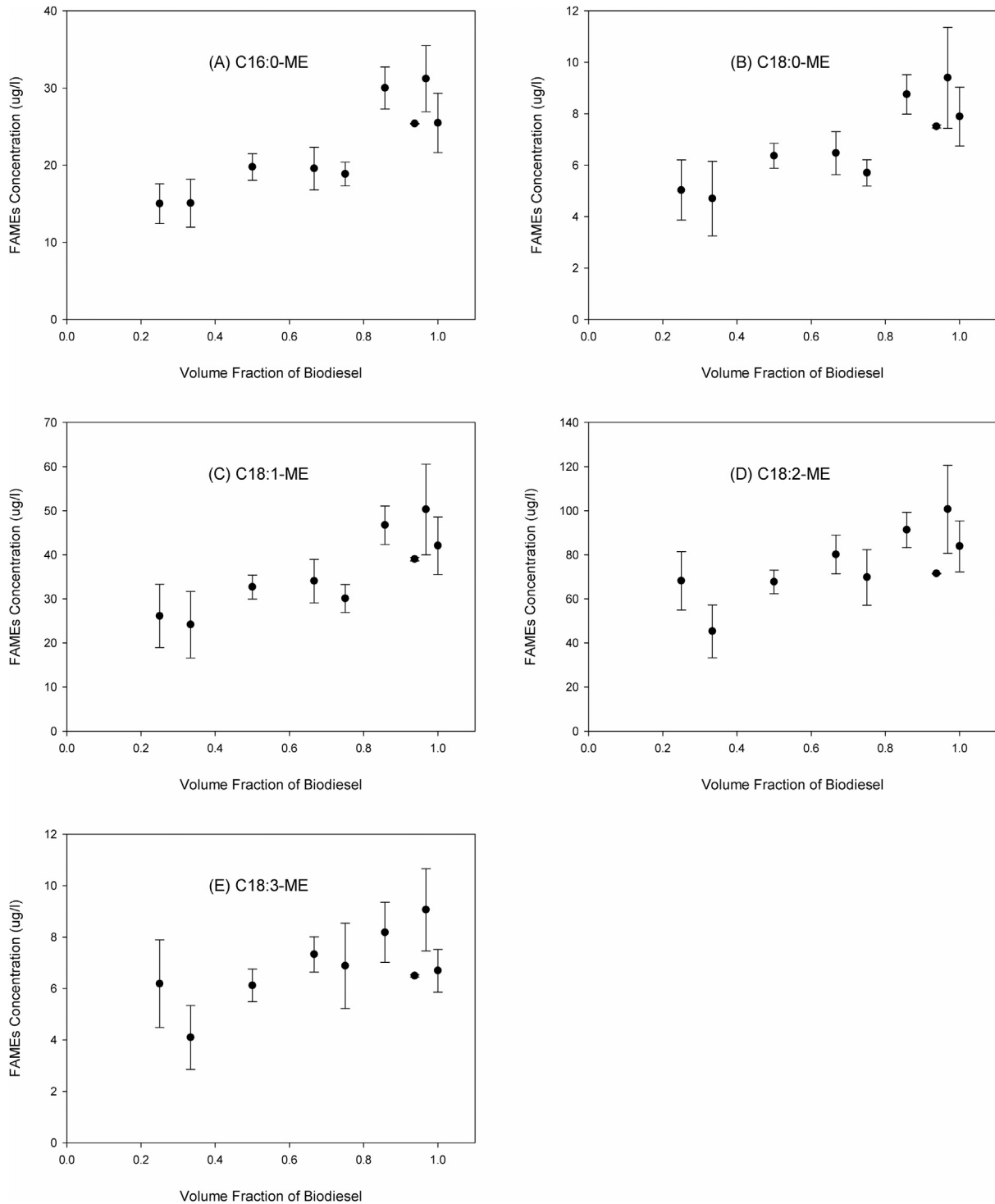


Fig. 7. WAF concentrations of FAMES in different biodiesel and diesel blends.

mobility (Miller and Mudge, 1997). The mechanism via which the petrodiesel inhibited the biodegradation of biodiesel was investigated in this study. The fundamentally different molecular structures of petrodiesel and biodiesel result in different macroscopic physicochemical properties for both fuels. Biodiesel has a higher viscosity and surface tension compared to petrodiesel. We conducted the partitioning experiment and found that the presence of petrodiesel appeared to affect the bioavailability of biodiesel due to the partitioning of biodiesel and petrodiesel in the aqueous phase. Fig. 7 presents the soluble FAME concentrations of biodiesel with different increasing loads of petrodiesel. Compared to 45  $\mu\text{l}$  pure biodiesel in 120 ml water, the partitioning of C16:0-ME, C18:0-ME, C18:1-ME, C18:2-ME and C18:3-ME slightly increased for the blended oil with 1.5  $\mu\text{l}$  petrodiesel added, then decreased. However, when petrodiesel loads increased up to 90  $\mu\text{l}$ , the concentration of soluble FAMES did not decrease. With further increase in the petrodiesel loads up to 135  $\mu\text{l}$ , the concentration of soluble FAMES slightly increased. This behavior showed the same trend as the methane production rate shown in Table 1. Both petrodiesel and biodiesel have very poor solubility in water, the effective oil–oil attraction induces segregation of the bulk oil from water. Chandler (2005) proposed that the effective oil–oil attraction that drives aggregation is actually a result of the strong water–water hydrogen bond attractive forces, which includes segregation of the oil from water. The free energy of solvating small hydrophobic species scales linearly with the volume of the solute. For a given biodiesel oil loads, increasing the loads of petrodiesel was capable of decreasing the dissolved concentrations of FAMES. Under this condition, in the presence of petrodiesel in the nonaqueous phase liquid had a negative effect on the dissolved concentrations of FAMES. If the FAMES mass transfer through the cell membrane is idealized according to the Fick's First Law of diffusion, lower petrodiesel loads in the blends, which had higher concentration of dissolved FAMES in water, would have a higher diffusion driving force across the cell membrane. Yassine et al. (2013b) studied the effect of the aqueous solubility of poorly soluble materials on their biodegradation rates under aerobic conditions, the higher the aqueous concentration of the compound, the higher is its bioavailability to the degrading populations. Therefore, in the presence of petrodiesel, the partitioning of FAMES in aquatic systems affects their biodegradation due to the bioavailability of FAMES.

#### 4. Conclusions

The goal of this study was to evaluate the methanogenic biodegradation rate of soybean biodiesel in the presence of different loads of petrodiesel. Biodiesel was observed to biodegrade to methane even in the presence of elevated concentrations of petrodiesel. Petrodiesel, however, was not biodegraded under methanogenic conditions. As for the effect of the presence of petrodiesel on the biodegradation of biodiesel, it affected the biodegradation rate due to the bioavailability of biodiesel in the aqueous phase. Both the biodegradation first order rate constant and methane production efficiency increased almost linearly with the increasing fraction of biodiesel. The biodegradation of biodiesel in BMP tests using biomass acclimated to biodiesel only was more sensitive to the presence of petrodiesel than when biomass acclimated to the presence of petrodiesel was used. The presence of

petrodiesel has a greater effect on the rate of biodegradation than the biodegradation efficiency.

#### Acknowledgment

Funding of this research was made possible through the U.S. Environmental Protection Agency (U.S. EPA) Oil Spill Research Program managed by the Land Remediation and Pollution Control Division of the National Risk Management Research Laboratory, Cincinnati, OH, under Contract No. EP-C-11-006, Work Assignment 3-19.

#### References

- Aktas, D.F., Lee, J.S., Little, B.J., Ray, R.I., Davidova, I.A., Lyles, C.N., Suffita, J.M., 2010. Anaerobic metabolism of biodiesel and its impact on metal corrosion. *Energy Fuels* 24 (5), 2924–2928.
- Chandler, D., 2005. Interfaces and the driving force of hydrophobic assembly. *Nature* 437 (7059), 640–647.
- Christopher, Lew P., Kumarc, Hemanathan, Zambared, Vasudeo P., 2014. Enzymatic biodiesel: challenges and opportunities. *Appl. Energy* 119, 497–520.
- Cyplik, P., Schmidt, M., Szulc, A., Marecik, R., Lisiecki, P., Heipieper, H.J., 2011. Relative quantitative PCR to assess bacterial community dynamics during biodegradation of diesel and biodiesel fuels under various aeration conditions. *Bioresour. Technol.* 102, 4347–4352.
- DeMello, J.A., Carmichael, C.A., Peacock, E.E., Nelson, R.K., Arey, J.S., Reddy, C.M., 2007. Biodegradation and environmental behavior of biodiesel mixtures in the sea: an initial study. *Mar. Pollut. Bull.* 54, 894–904.
- Gray, N.D., Sherry, A., Hubert, C., Dolfig, J., Head, I.M., 2010. Methanogenic degradation of petroleum hydrocarbons in subsurface environments: remediation, heavy oil formation, and energy recovery. *Adv. Appl. Microbiol.* 72 (C), 137–161.
- Gupta, M., Sharma, D., Suidan, M.T., Sayles, G.D., 1996. Biotransformation rates of chloroform under anaerobic conditions – I. Methanogenesis. *Water Res.* 30 (6), 1377–1385.
- Head, I.M., Jones, D.M., Larter, S.R., 2003. Biological activity in the deep subsurface and the origin of heavy oil. *Nature* 426 (6964), 344–352.
- Hill, J., Nelson, E., Tilman, D., Polasky, S., Tiffany, D., 2006. Environmental, economic, and energetic costs and benefits of biodiesel and ethanol biofuels. *Proc. Natl. Acad. Sci. U. S. A.* 103 (30), 11206–11210.
- Khan, N., Warith, M.A., Luk, G., 2007. A comparison of acute toxicity of biodiesel, biodiesel blends, and petrodiesel on aquatic organisms. *J. Air Waste Manag. Assoc.* 57 (3), 286–296.
- Lisiecki, P., Chrzanowski, Ł., Szulc, A., Ławniczak, Ł., Biatas, W., Dziadas, M., Owsianiak, M., Staniewski, J., Cyplik, P., Marecik, R., Jeleń, H., Heipieper, H.J., 2014. Biodegradation of diesel/biodiesel blends in saturated sand microcosms. *Fuel* 116, 321–327.
- Miller, N.J., Mudge, S.M., 1997. The effect of biodiesel on the rate of removal and weathering characteristics of crude oil within artificial sand columns. *Spill Sci. Technol. Bull.* 4 (1), 17–33.
- Owsianiak, M., Chrzanowski, L., Szulc, A., Staniewski, J., Olszanowski, A., Olejnik-Schmidt, A.K., Heipieper, H.J., 2009. Biodegradation of petrodiesel/biodiesel blends by a consortium of hydrocarbon degraders: effect of the type of blend and the addition of biosurfactants. *Bioresour. Technol.* 100 (3), 1497–1500.
- Pasqualino, J.C., Montané, D., Salvadó, J., 2006. Synergic effects of biodiesel in the biodegradability of fossil-derived fuels. *Biomass Bioenergy* 30 (10), 874–879.
- Prince, R.C., Haitmanek, C., Lee, C.C., 2008. The primary aerobic biodegradation of biodiesel B20. *Chemosphere* 71, 1446–1451.
- Schnepf, R., Yacobucci, B.D., 2013. Renewable Fuel Standards (RFS): Overview and Issues. CRS report for congress, pp. 1–31.
- Yassine, M.H., Wu, S., Suidan, M.T., Venosa, A.D., 2012. Microtox aquatic toxicity of petrodiesel and biodiesel blends: the role of biodiesel's autoxidation products. *Environ. Toxicol. Chem.* 31 (12), 2757–2762.
- Yassine, M.H., Wu, S., Suidan, M.T., Venosa, A.D., 2013a. Aerobic biodegradation kinetics and mineralization of six petrodiesel/soybean-biodiesel blends. *Environ. Sci. Technol.* 47 (9), 4619–4627.
- Yassine, M.H., Suidan, M.T., Venosa, A.D., 2013b. Microbial kinetic model for the degradation of poorly soluble organic materials. *Water Res.* 47 (4), 1585–1595.
- Zhang, X., Peterson, C., Reece, D., Haws, R., Möller, G., 1998. Biodegradability of biodiesel in the aquatic environment. *Trans. Am. Soc. Agric. Eng.* 41 (5), 1423–1430.